scientific reports

Check for updates

OPEN

Differences in cardiac mechanics assessed by left ventricular hemodynamic forces in athletes and patients with hypertension

Dinara Jumadilova[1], Yeltay Rakhmanov[1], Nail Khissamutdinov[2], Aizhan Zhankorazova[1], Bauyrzhan Toktarbay[1], Zaukiya Khamitova[1], Nurmakhan Zholshybek[1], Makhabbat Bekbossynova[2], Tairkhan Dautov[3], Abduzhappar Gaipov[1], Giovanni Tonti[4] & Alessandro Salustri[1]✉

We sought to assess cardiac magnetic resonance derived left ventricular hemodynamic forces (HDF) in athletes compared to patients with hypertension. Sixty athletes and 48 hypertensive patients were studied. HDF were measured during the entire cardiac cycle, the systolic phase, suction, early LV filling, and atrial thrust. Statistical comparisons were made between athletes and hypertensive patients, and between endurance and strength athletes. The slope of the systolic ejection was higher in athletes compared to hypertensive patients (541.5 vs. 435 1/sec; $p = 0.033$). Athletes showed higher HDF during the first phase of systole (4.53 vs. 3.86; $p = 0.047$) and the systolic impulse (11.26 vs. 8.76; $p = 0.045$). Compared to hypertensive patients, the AUC of the elastic rebound in athletes was lower (-0.31 vs. -0.44; $p = 0.011$). Moreover, hypertensive patients had an abnormal suction as revealed by a divergent direction (apex-to-base) of the HDF. The atrial thrust was higher in hypertensive patients than in athletes (-0.31 vs. -0.05; $p < 0.001$). Compared to endurance athletes, strength athletes had a shorter duration of the systolic impulse (250 vs. 280 ms; $p = 0.019$) and higher AUC during the early LV filling (1.65 vs. 0.97; $p = 0.016$). We conclude that HDF allows distinction between the hemodynamic patterns of athletes and patients with hypertension.

Keywords Hemodynamic forces, Intraventricular pressure gradients, Cardiovascular magnetic resonance, Athletes, Hypertension

Intensive exercise training induces left ventricular (LV) morphologic and functional adaptations referred to as "athletes' heart". Cross-sectional studies have demonstrated that training-induced LV remodelling is characterised by increased mass, wall thickness, and cavity diameter, which may differ in relation to the type of sport[1,2]. Moreover, conventional Doppler, pulsed-wave tissue Doppler and two-dimensional strain echocardiography have been applied in the characterization of hemodynamics of training-induced functional changes and to differentiate between physiological and pathological LV hypertrophy[3]. However, the conventional parameters that are commonly used (LV ejection fraction and Doppler indices of diastolic function) suffer from load dependency and low specificity, and despite a large body of data available in the literature there are still areas of uncertainty on the impact of the training-induced cardiac remodelling on the intraventricular hemodynamics[4]. In contrast, patients with arterial hypertension represent a clinical model of elevated afterload that may induce a pathological structural remodelling (concentric or eccentric LV hypertrophy) resulting in abnormal intraventricular pressure gradients (IVPG), which represent the consequence of LV deformation and play a central role in cardiac function that governs blood flow[5,6]. Thus, it would be important to analyse the IVPG in athletes and in hypertensive patients to detect the hemodynamic consequences and differentiate between physiological and pathological cardiac adaptation.

Noninvasive evaluation of the hemodynamic forces (HDF), using either particle imaging velocitometry echocardiography or 4-dimensional flow magnetic resonance imaging, has been proposed as a useful tool for

[1]School of Medicine, Nazarbayev University, 010000 Astana, Kazakhstan. [2]Heart Center, University Medical Center, 010000 Astana, Kazakhstan. [3]Clinical and Academic Department of Radiology and Nuclear Medicine, University Medical Center, 010000 Astana, Kazakhstan. [4]Department of Cardiovascular Disease, University G. D'Annunzio, Chieti-Pescara, Italy. ✉email: alessandro.salustri@nu.edu.kz

analysing the development of IVPG during the cardiac cycle and detect any derangement from the normal sequence which represents unequivocal indications of abnormal hemodynamics. However, despite its potential relevance, HDF analysis has not been part of the clinical diagnostic process so far due to the complexity of image acquisition, high cost and low availability.

Recently, a new method for estimating HDF from the tracking of the LV endocardial boundary has been proposed which overcomes the need for assessment of blood velocities inside the left ventricle[7]. The method correlates well to 4D flow magnetic resonance imaging (that represents the gold standard for evaluation of HDF)[8]and has been applied in several clinical scenarios[9,10]. However, no study has compared so far the HDF patterns in athletes with those in subjects with a pathological model of pressure overload as in arterial hypertension.

Based on these concepts, we sought to analyse the HDF pattern in athletes with the following aims: (1) To provide the range of normal values of HDF in athletes; (2) To compare the HDF in athletes with those in hypertensive patients; and (3) To compare the HDF in endurance vs. strength athletes.

Methods

Study population

The study was conducted at the Athletic Center of Nazarbayev University in collaboration with the Heart Center, University Medical Center in Astana, Republic of Kazakhstan. A group of athletes from Kazakhstan sport federations (triathlon and weightlifting) with unremarkable cardiovascular screening tests were enrolled. Exclusion criteria included a history of diabetes, claustrophobia, or other established contraindications to CMR. Due to technical reasons, we also excluded any subjects with body weight > 100 Kg who cannot be scanned by our CMR system.

Sixty athletes > 18 yrs were selected. Among these, 38 were elite endurance athletes and 22 were engaged in strength-based activities. The training protocols were different based on the specific nature of sport. Endurance athletes have a low-training period (before the competitive period) followed by intense aerobic isotonic dynamic exercise (peak training period) at an incremental workload of 70–90% of maximal heart rate. In particular, they perform 1 h/day of incremental long-distance swimming (3,000 m/day divided into a series of 400–800 m), 1 h/day of long distance running (10,000 m/day), and 1.5 h/day of cycling (45,000 m/day). On the other hand, strength athletes train throughout the year with anaerobic isometric static exercise at an incremental workload of 40–60% of maximal heart rate. In particular, their training protocol includes 0.5 h/day of aerobic exercises and 3 h/day of strength training (divided into a series of 60 min of weightlifting at a high workload with 10 min of short breaks and active recovery).

Forty-eight patients with a history of hypertension > 5 years were selected from the outpatient clinic. We excluded from the study hypertensive patients with co-existing coronary artery disease, moderate/severe valvular heart disease, previous cardiac surgery, cardiomyopathies, end-stage chronic kidney disease, stroke or TIA.

Demographic information, physical parameters (height, weight, heart rate, and blood pressure), and clinical assessments were systematically obtained by proficient and certified personnel. Body surface area (BSA) was computed utilising the DuBois formula (0.20247 × height (m) 0.725 × weight (kg) 0.425).

Ethics

The research adhered to the ethical standards outlined in the Declaration of Helsinki and received approval from the Ethical Committee of Nazarbayev University (NU-IREC #550/20042022). All participants signed an informed consent prior to the examination.

CMR acquisition

Cine CMR studies were performed at the Heart Center, University Medical Center, in Astana, Republic of Kazakhstan, using a Siemens Magnetom Avanto 1.5 Tesla machine. Endurance athletes were studied at peak training period, while strength athletes were studied at any time during the year. The CMR scanning protocol included standard cardiac sequences recommended by the European Association of Cardiovascular Imaging[11]. The localiser scans were acquired using True Fast Imaging with Steady-State Free Precession (TRUFI), multi 2Ch view, Institute for Personality and Ability Testing (IPAT), and four-chamber (4Ch) view. These were followed by white-blood image acquisitions in long-axis 4Ch-, 2Ch-, and 3Ch-, and short-axis views. For all acquisitions the distance factor was kept at 20% with a slice thickness of 8 mm, a repetition time (TR) of 34.68 ms, and an echo time (TE) of 1.22 ms. The acquired images were stored in the Picture Archiving and Communication System (PACS) and retrieved for off-line analysis.

Analysis of CMR images

All studies were anonymized and encoded with three random digits to maintain patient confidentiality and reduce bias. Thus, observers engaged in image analysis did not have access to participants' personal data.

Images were analysed by two observers (D.J. and N.K.) with > 6 years of experience in cardiac imaging using a dedicated software (Q Strain version 1.3.0.79; Medis, Leiden, the Netherlands) which allows to calculate HDF by visualising three routine long-axis and one short-axis cine randomly pre-selected images from PACS. To calculate basic parameters of LV function such as LV end-diastolic (EDV) and end-systolic volumes (ESV), ejection fraction (EF), stroke volume (SV), and cardiac output (CO), long axis slices were used. The volume measurement was based on tracing of endocardial contours at end-diastolic (ED) and end-systolic (ES) frames. For measurements of the LV mass, tracing of the epicardial contours was added. This allows the software to calculate the weight of the myocardium, including the papillary muscles, at end-diastole. While LV volumes are

analysed using long axis views obtained in three standard directions, the LV mass is conventionally measured from short axis views.

The algorithm for calculation of the HDF is based on a mathematical model by Pedrizzetti el al[7]:

$$F(t) = \rho \int_{S(t)} \left[x \left(\frac{\partial v}{\partial t} * n \right) + v (v * n) \right] dS$$

To perform HDF analysis, a 2, 3, and 4-chamber cine image is needed. After the selection of the optimal slice, consecutive cardiac frames on each long-axis view were reviewed to select the ED and ES frames. The ED frame was selected when the LV myocardium is maximally relaxed (no further outward movement) and the ventricular cavity is the largest, while mitral leaflets are open but ready to close in the next frame of cardiac cycle. Similarly, the ES frame was selected when the LV myocardium is maximally contracted (no further inward movement) and the ventricular cavity is the smallest while aortic leaflets are open but ready to close in the next frame. Then, the LV endocardial border was automatically detected by the software in the appropriate cardiac frame. The observers had the freedom to manually change the endocardial borders automatically selected by the program, if needed. The endocardial contouring feature allowed the calculation of standard volumetric parameters (such as the LV volumes and EF), which are dependent on endocardial border detection.

Finally, the calculation of the LV HDF requires measurements of the mitral valve area (MVA) and aortic valve area (AVA). The MVA was calculated from the measurement of the mitral annulus diameter ($A = \pi\ [d/2]^2$) and the measurements were performed after the observers selected the appropriate cardiac frame with maximal MV opening. The MVA was calculated from the 4Ch and 2Ch views at ED frame and the mean of the two values were considered. The AVA was calculated from the aortic annulus diameter in the 3Ch view at ES frame from the inner-edge to the inner-edge of the valve leaflets. For each structure (MV and AV), three measurements of the diameters were performed, and the values were averaged and inserted manually into the software for automatic calculation of the MVA and AVA.

HDF parameters

In the normal left ventricle, HDF occurs in the longitudinal (apical-base, A-B) and transversal (lateral-septal, L-S) planes, with the longitudinal direction being the most predominant force. The longitudinal direction of the forces is depicted as a curve that deflects positively when HDF is directed toward the LV base and negatively when it is directed toward the LV apex. The Newton (N) is the unit of force. The value of HDF is divided by the fluid density and gravity acceleration after being initially normalised by the LV volume. This makes it possible to describe the acceleration due to gravity as a percentage (dimensionless) and makes it easier to compare subjects. Overall HDF is given as root mean square (RMS) over the entire cardiac cycle, considering both absolute values (regardless of whether these values were positive or negative). Parameters with either a positive or negative value are given as area under the curve (AUC, %) derived from the hemodynamic power curves[12]. For the purpose of the study, the following phases of the cardiac cycle were identified (Fig. 1):

1. *HDF along the entire cardiac cycle* expresses in RMS as the mean amplitude of the forces along the entire cardiac cycle. The following parameters were calculated:
    a. A-B (longitudinal) HDF, %.
    b. L-S (transversal) HDF, %.
    c. L-S/A-B ratio.
    d. Average angle of the force (representing the dominant force vector during the entire cardiac cycle ranging from 90°, when the force is perfectly along the base-apex direction, to 0°).
2. *Slope of the systolic ejection* (Fig. 1. Panel A) measures the ability of the ventricle to generate a high-pressure gradient quickly. The slope was identified as the tangent to the ascending phase of the systolic impulse starting from the point where the HDF curve changes direction and becomes positive. It is expressed as 1/Sec.
3. *First phase of the systole* (Fig. 1. Panel B) represents how the LV changes its volume over time, measured from the initial change in the dV/dt curve to the next change in the direction of the dV/dt curve (that corresponds to the peak of the HDF curve). The following parameters were calculated:
    a. Hemodynamic work (AUC), %.
    b. Duration, ms.
    c. Peak HDF, %.
4. *Systolic phase* (Fig. 1. Panel C) includes force generation and decay, characterised by apex-to-base and base-to-apex IVPG. It starts when the dV/dt curve changes to negative and ends when the curve flattens after the systolic rebound on the HDF curve. Since this phase includes both positive *(systolic impulse)* and negative *(elastic rebound)* HDF components, which are related to different hemodynamic patterns, each component was analysed separately using the following parameters:
    a. Hemodynamic work (AUC), %.
    b. Duration, ms.
5. *Suction* (Fig. 1. Panel D) starts at the end of myocardial fiber contraction. During this phase, there are no changes in LV volume, but IVPG are generated due to changes in the LV shape. It starts when the dV/dt curve

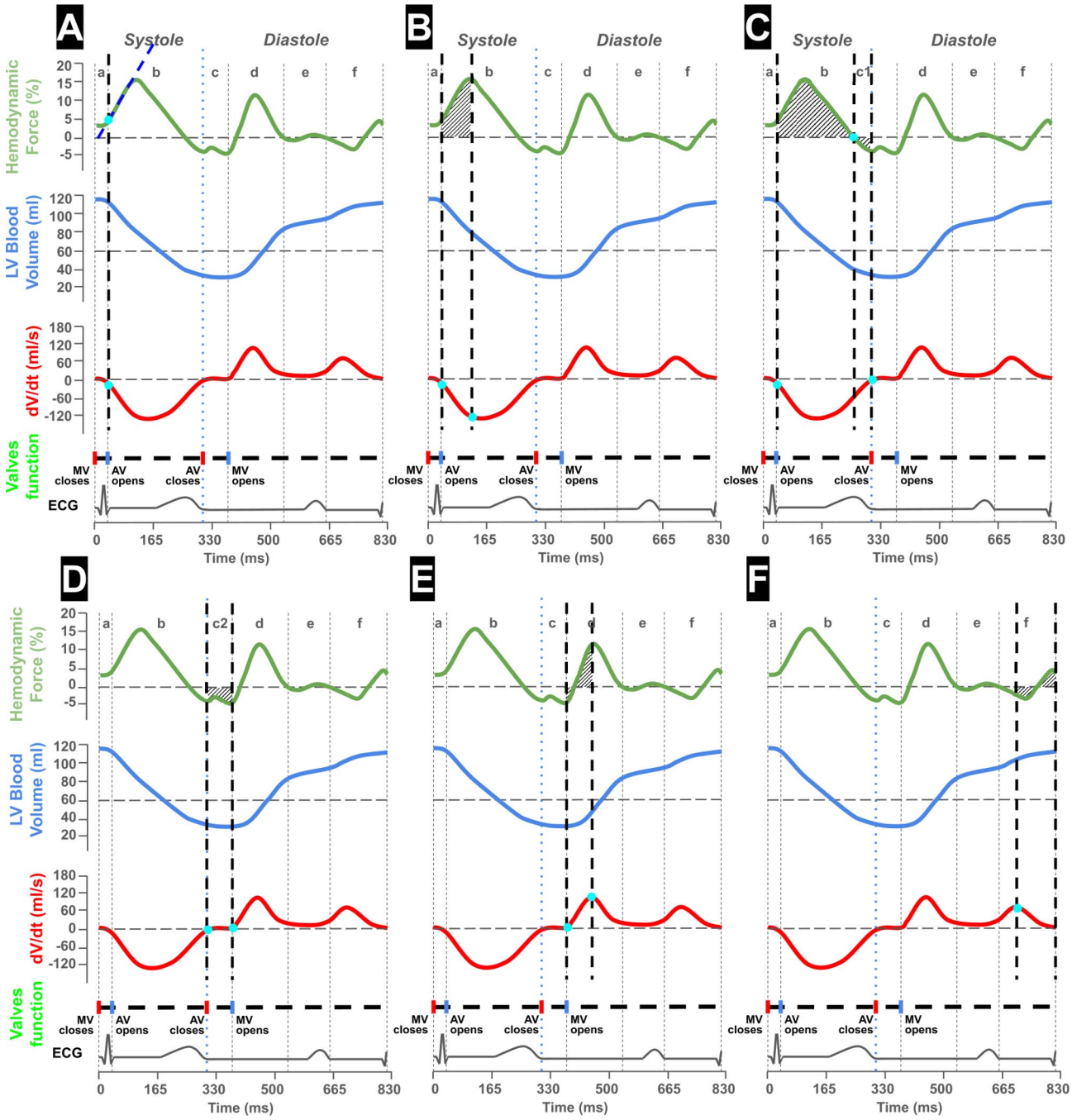

Fig. 1. Events of the cardiac cycle considered for hemodynamic forces analysis. Each panel (**A** to **F**) represents the hemodynamic forces (green), volumes (blue), dV/dt (red), valves opening/closure time, and ECG. The vertical dotted lines represent the time selected from the dV/dt curve. Panel A: Slope of the systolic ejection; Panel B: First phase of the systole; Panel C: Systolic phase (including systolic impulse and elastic rebound); Panel D: Suction; Panel E; Early filling of the left ventricle; Panel F: Atrial thrust.

changes its direction after reaching the smallest LV volume and ends at the next directional change, after a relatively flat period, corresponding to early LV filling. Metric included:

a. Hemodynamic work (AUC), %.

6. *Early filling of the left ventricle* (Fig. 1. Panel E) was measured from the point where the dV/dt curve changes direction post-suction till the next negative change at the peak of the curve. Metric included:

a. Hemodynamic work (AUC), %.

7. *Atrial thrust* (Fig. 1. Panel F) was measured from the last positive peak where the dV/dt curve changes direction from positive to negative until the end of the cardiac cycle (Q wave on the ECG). Metric included:

   a. Hemodynamic work (AUC), %.

Statistics

The statistical analysis was conducted using Stata version 18.0 (STATA, StataCorp, Texas, US). Univariate normality assumptions were validated through the Shapiro-Wilk test. Continuous variables were reported as mean ± SD and subjected to comparison using Student's t-test or the Mann–Whitney rank sum test for unpaired comparisons, as deemed appropriate. For non-normally distributed values, medians and interquartile ranges (IQR) were utilised. Categorical variables were expressed as counts and percentages and subjected to comparison using the χ^2 test or Fisher's exact test, as appropriate. A significance level of 0.05 was used for all statistical tests.

Intra-observer and intra-observer variability were evaluated in a randomly selected sample of 25 athletes. Two investigators independently conducted measurements of the same examination, and one investigator repeated the analysis after 10 days blinded to prior measurements. In terms of inter-observer variability, there was a good correlation for the longitudinal and transverse HDF (ICC 0.85 [0.67–0.93] and 0.86 [0.69–0.94], respectively; $p < 0.001$ for both). For intra-observer variability, longitudinal and transverse HDF showed excellent correlation (ICC 0.91 [0.78–0.93] and 0.93 [0.83–0.97], respectively; $p < 0.001$for both)[13].

A sample size calculation was conducted prior to study enrolment resulting in a power in excess of 80% and significance level of 0.05 by using the following formula:

$$N = \frac{(r+1)(Z_{\frac{\alpha}{2}} + Z_{1-\beta})^2 \sigma^2}{r(\mu_1 - \mu_2)^2}$$

where N is the sample size, $Z_{\alpha/2}$ is Z-score for the level of significance (1.96), $Z_{1-\beta}$ is Z-score for the desired power of 0.80 (0.84), r is ratio of the sample size (N1/N2), σ^2 is pooled standard deviation and $(\mu_1 - \mu_2)$ is the mean difference between groups.

Role of the funding source

This study was funded by a grant of the Ministry of Education and Science of the Republic of Kazakhstan, № AP14869730. The sponsor had no role in study design; in the collection, analysis, and interpretation of data; in the writing of the report; and in the decision to submit the paper for publication.

Results

Subject characteristics are summarised in Table 1. Athletes had a sport experience of 10 ± 7 years, were younger, had lower heart rate and lower blood pressure. The mean duration of hypertension was 11 ± 2 years. Female gender was prevalent among hypertensive patients compared to athletes (60% vs. 25%, respectively; $p = 0.001$).

BSA, Body Surface Area; DBP, diastolic blood pressure; HR, heart rate; MAP, mean arterial pressure; SBP, systolic blood pressure.

Conventional CMR parameters

Conventional CMR parameters are reported in Table 2. LVEF was slightly higher in hypertensives compared to athletes (71.4% vs. 65.7%, respectively; $p < 0.001$). Compared to hypertensives, athletes had larger LV volumes and SV, and higher LV mass.

	Athletes ***n*** **= 60**	**Hypertensives** ***n*** **= 48**	***P*-value**
Age (yrs)	33 (29;38)	56 (44;63)	< 0.001
Weight (kg)	75 ± 15	79 ± 13	0.236
Height (cm)	176 (170;180)	165 (158;170)	< 0.001
BSA (m^2)	1.93 (1.75;2.07)	1.93 (1.74;2.05)	0.776
HR (bpm)	63 (58;70)	74 (71;78)	< 0.001
SBP (mmHg)	119 ± 12	138 ± 15	< 0.001
DBP (mmHg)	78 ± 11	93 ± 10	< 0.001
MAP (mmHg)	91 ± 10	109 ± 11	< 0.001
Sport experience (yrs) Duration of hypertension (yrs)	10 ± 7	11 ± 2	
Male/Female, n (%)	45/15 (75)	19/29 (40)	0.001

Table 1. General characteristics of the study groups.

Parameters	Athletes $n=60$	Hypertensives $n=48$	*P*-value
LVEF (%)	65.7 (61.9;71.8)	71.4 (67.5;76.0)	0.001
LVEDV (mL)	142 ± 33	101 ± 21	< 0.001
LVEDVi (mL/m^2)	75.0 ± 16.0	53.4 ± 10.3	< 0.001
LVESV (mL)	47 (34; 61)	30 (22; 38)	< 0.001
LVESVi (mL/m^2)	24.5 (18.5;30.4)	15.3 (12.4;18.8)	< 0.001
LVM (g)	155.4 ± 38.8	130.8 ± 31.2	< 0.001
LVMi (g/m^2)	81.2 ± 16.1	68.5 ± 12.2	< 0.001
SV (mL)	94 ± 20	71 ± 17	< 0.001
SVi (mL/m^2)	49.5 ± 10.4	37.4 ± 8.3	< 0.001
AAD (mm)	23.4 (21.6;25.3)	21.4 (20.2;23.3)	0.009
MAD (mm)	35.8 ± 3.6	33.8 ± 3.5	0.002

Table 2. CMR parameters. AAD, Aortic annulus diameter; LVEF, Left ventricular ejection fraction; LVEDV, Left ventricular end-diastolic volume; LVEDVi:, Left ventricular end-diastolic volume indexed; LVESV, Left ventricular end-systolic volume; LVESVi, Left ventricular end-systolic volume indexed; MAD, Mitral annulus diameter; SV, Stroke volume; SVi, Stroke volume indexed.

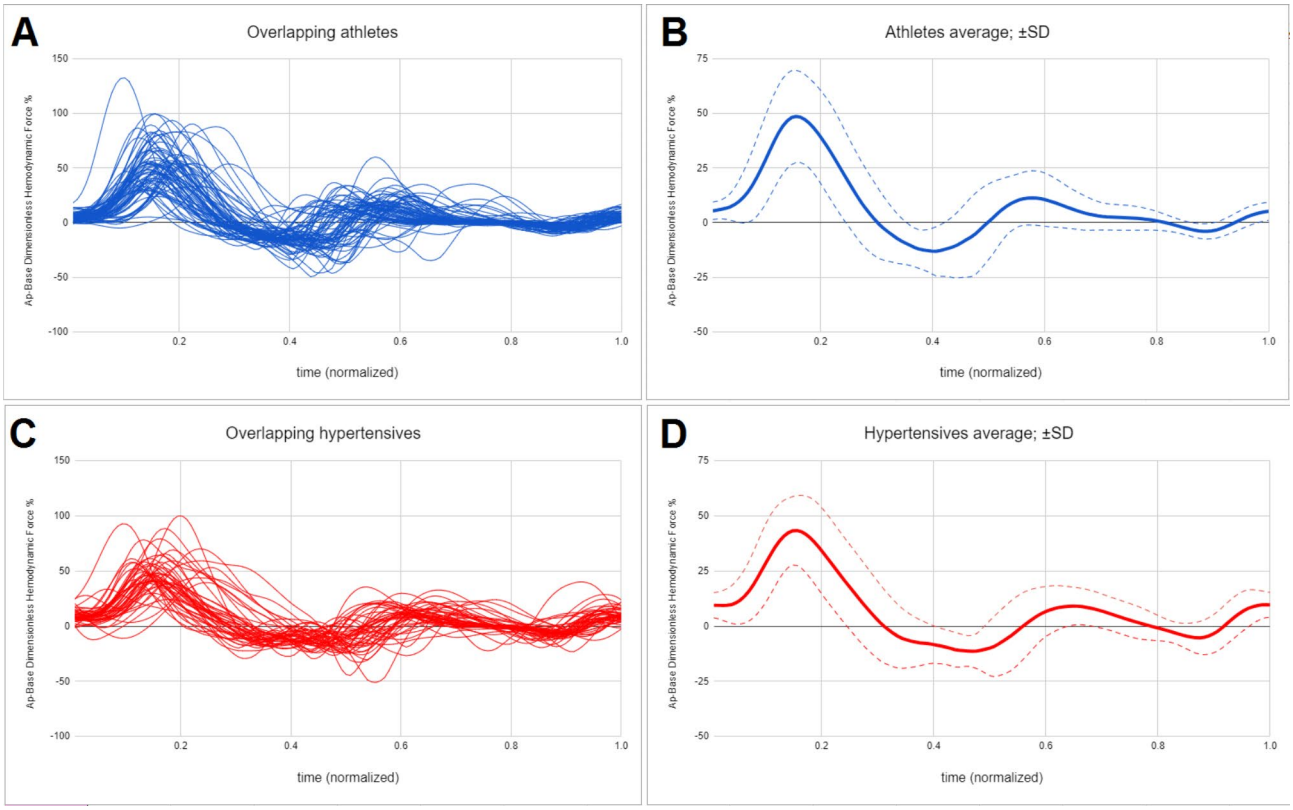

Fig. 2. Time profile of the HDF along the longitudinal axis (apex-to-base). Curves are displayed for individuals (A and C) and averaged (± SD) values (B and D), in athletes (top) and hypertensive patients (bottom). The HDF shows a positive systolic peak followed by a negative curve that includes the elastic rebound and the suction. The last two curves represent the hemodynamic patterns during diastole (positive: early left ventricular filling; negative: atrial thrust).

Hemodynamic forces

HDF along the entire cardiac cycle

Time profiles of the longitudinal HDF for individuals and as averaged (± SD) values are displayed in Fig. 2. Visual comparison of averaged HDF between the two groups shows lower systolic peak, prolonged early diastolic phase, and increased atrial thrust in patients with hypertension.

Parameters	Athletes $n=60$	Hypertensives $n=48$	*P*-value
A-B (%)	20.4 (16.8;26.0)	16.8 (15.8;21.2)	0.031
L-S (%)	3.9 (3.0;4.5)	3.7 (2.8;4.2)	0.099
L-S/A-B ratio (%)	19.3 ± 5.0	19.8 ± 5.2	0.636
Average Angle (°)	73.4 ± 3.1	73.8 ± 3.3	0.684

Table 3. Hemodynamic forces along the entire cardiac cycle.

Parameters	Athletes $n=60$	Hypertensives $n=48$	*P*-value
Slope of the systolic ejection			
Slope	541.5 (387.5;716.5)	435 (327;548)	0.033
First phase of the systole			
AUC, %	4.53 (3.43;6.09)	3.86 (3.19;4.77)	0.047
Duration, ms	148 ± 34	142.7 ± 31.4	0.405
Peak, %	62.9 (48.2;75.5)	46.8 (40.7;58.4)	0.001
Systolic Impulse			
AUC, %	11.26 (7.23;14.47)	8.76 (6.87;12.57)	0.045
Duration, ms	255 (236.5;306)	265 (238;291)	0.582
Elastic rebound			
AUC, %	-0.31 (-0.48;-0.16)	-0.44 (-0.70;-0.23)	0.011
Duration, ms	51.6 ± 18.7	70.1 ± 20.8	< 0.001
Suction			
AUC, %	-0.01 (-0.16;0.15)	0.09 (-0.06;0.21)	0.043
Early filling of the left ventricle			
AUC, %	1.12 (0.64;1.77)	1.33 (0.62;1.93)	0.804
Atrial thrust			
AUC, %	-0.05 (-0.11;-0.02)	-0.31 (-0.53;-0.15)	< 0.001

Table 4. Hemodynamic forces during selected phases of the cardiac cycle.

Hemodynamic forces values for the entire heart beat are reported in Table 3. Athletes had higher values of longitudinal HDF compared to hypertensive patients (20.4 vs. 16.8; $p=0.031$). No differences were detected in transversal HDF, ratio, and average angle between the two groups.

We divided athletes and hypertensive patients according to the mean age of each group, and we found that the difference in longitudinal HDF was nonsignificant between the elder half of athletes and the younger half of the hypertensive patients (20.0 vs. 19.2, p = ns). In contrast, we found a larger difference between the younger half of athletes and the elder half of the hypertensive patients (23.5 vs. 17.8, $p=0.008$). However, the duration of hypertension was longer in the older compared to the younger half of the hypertensive patients (15 vs. 8 years).

HDF of the single phases of the cardiac cycle

The comparative analysis of HDF parameters of the selected time intervals of the cardiac cycle in the two groups are reported in Table 4.

Athletes had a significantly higher slope of systolic ejection compared to hypertensive patients (541.5 vs. 435 1/sec, respectively; $p=0.033$). During the first part of the systole, compared to hypertensive patients, athletes generated a higher HDF (4.53 vs. 3.86, respectively; $p=0.047$) and a higher peak value (62.9 vs. 46.8, respectively; $p=0.001$). Moreover, athletes had a higher hemodynamic work during the systolic impulse (AUC 11.26 vs. 8.76, respectively; $p=0.045$), suggesting the development of higher pressure gradients during this phase of the cardiac cycle.

During the elastic rebound, compared to hypertensive patients, athletes generated a lower hemodynamic work (AUC −0.31 vs. -0.44, respectively; $p=0.011$) in a shorter period of time (51.6 vs. 70.1 ms, respectively; $p<0.001$). Moreover, while the mean value of hemodynamic work during suction was negative in athletes, hypertensive patients had a positive mean value (AUC −0.01 vs. 0.09, respectively; $p=0.043$), suggesting lack of efficacy of this hemodynamic mechanism in hypertensive patients. There were no differences in the early filling of the LV between the two groups, while the atrial thrust was significantly higher (more negative values) in hypertensive patients compared to athletes (AUC −0.31 vs. -0.05, respectively; $p<0.001$), indicating the importance of the atrial component in the LV filling in hypertensive patients.

Parameters	Endurance $n=38$	Strength $n=22$	*P*-value
A-B (%)	20.8 (18.3;26.9)	19.9 (13.8;24.5)	0.462
L-S (%)	4.04 (3.17;4.51)	3.84 (3.06;5.16)	0.921
L-S/A-B HDF ratio (%)	18.6 ± 4.5	20.6 ± 5.7	0.153
Average Angle (°)	73.3 ± 2.9	73.5 ± 3.5	0.861

Table 5. Endurance vs. strength athletes (HDF analysis along the entire cardiac cycle).

Parameters	Endurance $n=38$	Strength $n=22$	*P*-value
Slope of the systolic ejection			
Slope	541.5 (392;673)	527 (356;771)	0.752
First phase of the systole			
AUC, %	4.53 (3.67;6.00)	4.55 (2.53;6.28)	0.607
Duration, ms	147 (135;171)	133 (118;148)	0.007
Peak, %	65.5 ± 19.5	60.4 ± 22.7	0.365
Systolic Impulse			
AUC, %	11.26 (7.84;14.53)	11.55 (5.51;14.41)	0.634
Duration, ms	280 ± 51	250 ± 35	0.019
Elastic rebound			
AUC, %	-0.34 ± 0.23	-0.32 ± 0.19	0.646
Duration, ms	51.7 ± 16.0	51.5 ± 23.1	0.977
Suction			
AUC, %	0.03 (-0.13;0.19)	-0.05 (-0.19;0.09)	0.244
Early filling of the left ventricle			
AUC, %	0.97 (0.51;1.42)	1.65 (0.90;2.72)	0.016
Atrial thrust			
AUC, %	-0.04 (-0.09;-0.01)	-0.06 (-0.15;-0.02)	0.225

Table 6. Endurance vs. strength athletes (HDF during selected phases of the cardiac cycle).

HDF in endurance vs. strength athletes

Compared to strength athletes, endurance athletes had higher LVMi (86.4 ± 15.3 vs. 71.8 ± 21.7; $p=0.008$) and LVEDVi [76.3 vs. 68.2, respectively; $p=0.004$)]. Comparative analysis between endurance and strength athletes are reported in Tables 5 and 6. There were no differences in the HDF along the entire heart beat (Table 5). The duration of the first phase of systole and the duration of the systolic impulse were shorter in strength compared to endurance athletes (133 vs. 147 ms; $p=0.007$; 250 vs. 280 ms; $p=0.019$, respectively). Additionally, the AUC of the early filling of the left ventricle was lower in endurance compared to strength athletes (0.97 vs. 1.65, respectively; $p=0.016$).

Discussion

The main goal of our study was to compare the exercise-induced physiological adaptation of the heart to the pathological hemodynamic changes induced by pressure overload in hypertensive patients using LV HDF derived from feature-tracking CMR. We had three primary objectives: (1) To provide the range of normal values of HDF in athletes; (2) To compare the HDF in athletes with those in patients with uncomplicated hypertension; and (3) To compare the HDF in endurance vs. strength athletes.

The results of the present study provide reference values for athletes, not only for the entire heart beat but also for single time intervals corresponding to the different phases of the cardiac cycle. In addition, HDF analysis was able to provide insights into the different hemodynamic changes induced by physiological physical training compared to a pathological model of increased LV afterload due to hypertension. Finally, when comparing the different types of training, strength athletes had shorter duration of the systolic impulse and higher HDF of the early LV filling, but no changes in the hemodynamic work.

We employed feature-tracking CMR imaging to measure non-invasively the IVPG which has a fundamental role in cardiac adaptation. HDF analysis, which corresponds to the global value of IVPG integrated over the ventricular volume, can identify the hemodynamic pattern associated with adaptation to different pressure overload at an earlier stage compared to LVEF and deformation analysis. While previous methods for HDF analysis were hampered by low feasibility[14]. The method we have applied for HDF analysis is based on a new mathematical model that integrates knowledge of LV geometry, endocardial tissue movement, and the dimensions of the aortic and mitral orifices[7]. These parameters may affect blood velocity and the mass in motion

(momentum), which can impact ventricular remodeling and calculation of HDF, however normalisation of HDF by LV volume facilitates comparisons of HDF between ventricles of different sizes.

HDF analysis has been already applied in several studies, using either CMR or echocardiography, including normal subjects[15–17], athletes[18], patients with different types of pathologies (such as heart failure[19–25], cardiac resynchronization therapy[26,27], post-aortic coarctation[28]), and for the assessment of diastolic dysfunction[29]. However, as for most of the new techniques, standardisation of HDF measurements is still lacking, and different parameters have been reported in different studies. We believe that a detailed analysis of HDF during the phases of the cardiac cycle would provide insights into the complex mechanisms of cardiac function and characterise in detail the pathophysiological patterns in different cardiac adaptive models. The analysis of the HDF curves throughout the entire heart beat integrates in a single value all the components of the different phases of a cardiac cycle, and is not able to resolve the individual component. In fact, the results will include the mathematical sum of all the events (positive and negative directions) during the cardiac cycle, and cannot distinguish the HDF behaviour during a specific time interval. To overcome this limitation, we detected early changes in blood flow acceleration from the dV/dt curve and identified the time limits of all the phases of the cardiac cycle, including for example the elastic rebound and the suction period, which allows to quantify and compare the hemodynamic work of each phases of the cardiac cycle.

There is scanty data on HDF in athletes. Arvidsson et al. applied 4D flow magnetic resonance imaging to 14 elite athletes and 25 healthy volunteers[18]. Apart from the different methodology applied, they considered volume-normalised RMS force during systole, early, and late diastole. When compared to normal volunteers, they found no differences between controls and athletes. Preliminary data by Filomena et al. in mixed athletes[30] are consistent with our findings. However, they analysed HDF only for the entire cardiac cycle, the systolic phase, and the diastolic phase, while analysis of the different phases of the cardiac cycle was not considered.

The results from our study provide significant insights into the LV hemodynamics in athletes. When we analysed the entire cardiac cycle, longitudinal HDF was higher in athletes compared to hypertensive patients, while the transverse HDF, L-S/A-B ratio and the average angle were similar between the two groups (see Table 3). This indicates that athletes and hypertensive patients have the same (normal) orientation of the HDF, albeit with higher apex-to-base oriented IVPG in athletes. Analysis of the HDF curves during the different phases of the cardiac cycle indicates that athletes have a steeper slope of the systolic ejection, and higher peak/higher hemodynamic work during the first phase of systole. These data suggest the development of higher pressure gradients in a short period of time in athletes compared to hypertensive patients. In terms of diastolic function, compared to hypertensive patients, athletes had a less negative AUC values (-0.31 vs. -0.44, respectively; $p = 0.011$) and a shorter duration of the elastic rebound (51.6 vs. 70.6 ms, respectively; $p < 0.001$). This can be explained by the stiffness of the left ventricle in hypertensive patients which needs higher work and longer time to release the elastic energy stored by the preceding systolic deformation. In addition, this method allowed us to evaluate the suction that plays a major role in LV filling. Our results indicate that in hypertensive patients the suction mechanism is lost as demonstrated by the abnormal direction (apex-to-base) of the HDF during this phase. This might be related to an abnormal rate of untwisting in early diastole, a mechanism which has been shown to contribute to the occurrence of diastolic suction. Finally, while the early LV filling is similar, the atrial thrust is significantly higher in hypertensive patients than in athletes (-0.31 vs. -0.05, respectively; $p < 0.001$), indicating the importance of the active LV filling in hypertensive patients.

A previous study in a healthy volunteers demonstrated a weak decline of HDF parameters with age[16]. Since there is a significant difference in age between athletes and hypertensive patients in our population, the differences in HDF that we have found between the two groups could be simply related to age. However, the analysis of Faganello et al.[16] showed that a decline in HDF parameters is present only in subjects > 60 years, while the differences between subjects in the range 16–39 years vs. 40–59 years were statistically not significant. The mean age of our athletes (33 years) fits in the category 16–39 years, while the mean age of hypertensive patients (56 years) in the 40–59 years category of those reference values[16]. Thus, we should not expect significant age-related differences of HDF between our two groups. Rather, the difference we have found in HDF between athletes and hypertensive patients could be related to the effect of training and/or subclinical myocardial dysfunction in hypertensive patients, which would induce abnormal IVPG. We have also performed a subgroup analysis according to age and we found that the difference between the elder half of athletes and the younger half of patients with hypertension was smaller than the younger part of athletes and the elder part of patients with hypertension. However, this can be due to the longer duration of hypertension in the elder compared to younger half of the patients with hypertension (15 vs. 8 years, respectively).

Comparative analysis between endurance and strength athletes found no significant difference in HDF values along the entire heart beat. Analysis of the single phases of the cardiac cycle showed that strength athletes have a shorter duration of the first phase of the systole and of the systolic impulse. These findings can be explained by the different modalities of generation of IVPG in the two types of exercise, and suggest that strength athletes need less time to reach the systolic peak and generate the same level of hemodynamic work. Additionally, the early filling of the left ventricle was lower in endurance athletes compared to strength athletes. This finding could be explained by the higher LVMi and LVEDVi in endurance athletes, which may affect the LV untwisting and filling.

Study limitations

In our study population, 23% of the hypertensive patients had LVMi higher than the upper normal limits reported by Kawel-Boehm et al.[31]. The relatively low number of hypertensive patients with significant increase in LV mass can be explained by the exclusion of patients with hypertension-related complications, and is in line with the prevalence of LV hypertrophy reported in previous study[32]. The CMR protocol did not include the use of gadolinium contrast medium which prevents the assessment of myocardial fibrosis. In this regard, further

studies might address the relation between late gadolinium enhancement and the development of abnormal IVPG. Finally, we acknowledge that a study design which had included an age-matched healthy control group would have been desirable, however we aimed to compare athletes vs. hypertensive patients for differentiating HDF in two different models of LV remodeling (physiological vs. pathological).

Conclusions

HDF provide insights into intracardiac pressure dynamics and clearly distinguish between athletes and patients with uncomplicated hypertension. These results indicate the potential use of HDF as a noninvasive tool for distinguishing physiological from pathological cardiac adaptation.

Data availability

We confirm that all relevant data within the manuscript and all data underlying the findings are fully available without restriction from the corresponding author at the Nazarbayev University School of Medicine/University Medical Center in Astana for researchers who meet the criteria for confidential data.

Received: 26 July 2024; Accepted: 31 October 2024
Published online: 09 November 2024

References

1. Flanagan, H. et al. The athlete's heart: Insights from echocardiography. *Echo Res. Pract.* **10**, 15 (2023).
2. Hellsten, Y. & Nyberg, M. Cardiovascular adaptations to exercise training. *Compr. Physiol.* **6**, 1–32 (2011).
3. Simsek, Z. et al. Analysis of athletes' heart by tissue doppler and strain/strain rate imaging. *Int. J. Cardiovasc. Imaging*. **27**, 105–111 (2011).
4. La Gerche, A. et al. The athlete's heart—challenges and controversies: JACC focus seminar 4/4. *JACC*. **80**, 1346–1362 (2022).
5. Vos, J. L. et al. CMR-derived left ventricular intraventricular pressure gradients identify different patterns associated with prognosis in dilated cardiomyopathy. *Eur. Heart J. Cardiovasc. Imaging* **24**, 1231–1240 (2023).
6. Pedrizzetti, G., La Canna, G., Alfieri, O. & Tonti, G. The vortex—An early predictor of cardiovascular outcome? *Nat. Rev. Cardiol.* **11**, 545–553 (2014).
7. Pedrizzetti, G. On the computation of hemodynamic forces in the heart chambers. *J. Biomech.* **95**, 109323 (2019).
8. Pedrizzetti, G. et al. On estimating intraventricular hemodynamic forces from endocardial dynamics: A comparative study with 4D flow MRI. *J. Biomech.* **60**, 203–210 (2017).
9. Vallelonga, F. et al. Introduction to hemodynamic forces analysis: Moving into the new frontier of cardiac deformation analysis. *J. Am. Heart Assoc.* **10**, e023417 (2021).
10. Aimo, A. et al. Assessing cardiac mechanics through left ventricular haemodynamic forces. *Eur. Heart J. Imaging Methods Pract.* **2**, qyae077 (2024).
11. Messroghli, D. R. et al. Clinical recommendations for cardiovascular magnetic resonance mapping of T1, T2, T2* and extracellular volume: a consensus statement by the society for cardiovascular magnetic resonance (SCMR) endorsed by the European association for cardiovascular imaging (EACVI). *J. Cardiovasc. Magn. Reson.* **19**, 75 (2016).
12. Pedrizzetti, G., Faganello, G., Croatto, E. & Di Lenarda, A. The hemodynamic power of the heart differentiates normal from diseased right ventricles. *J. Biomech.* **119**, 110312 (2021).
13. Ismailov, T. et al. Reliability of left ventricular hemodynamic forces derived from feature-tracking cardiac magnetic resonance. *PLoS One*. **19**, e0306481 (2023).
14. Töger, J. et al. Hemodynamic forces in the left and right ventricles of the human heart using 4D flow magnetic resonance imaging: phantom validation, reproducibility, sensitivity to respiratory gating and free analysis software. *PLoS One* **13**, e0195597 (2018).
15. Ferrara, F. et al. Reference ranges of left ventricular hemodynamic forces in healthy adults: A speckle-tracking echocardiographic study. *J. Clin. Med.* **10**, 5937 (2021).
16. Faganello, G. et al. A new integrated approach to cardiac mechanics: Reference values for normal left ventricle. *Int. J. Cardiovasc. Imaging* **36**, 2173–2185 (2020).
17. Yang, W. et al. Unravelling the intricacies of left ventricular haemodynamic forces: Age and gender-specific normative values assessed by cardiac MRI in healthy adults. *Eur. Heart J. Cardiovasc. Imaging*. **25**, 229–239 (2024).
18. Arvidsson, P. M. et al. Left and right ventricular hemodynamic forces in healthy volunteers and elite athletes assessed with 4D flow magnetic resonance imaging. *Am. J. Physiol. Heart Circ. Physiol.* **312**, H314-H328 (2017).
19. Eriksson, J., Bolger, A. F., Ebbers, T. & Carlhäll, C. J. Assessment of left ventricular hemodynamic forces in healthy subjects and patients with dilated cardiomyopathy using 4D flow MRI. *Physiol. Rep.* **4**, e12685 (2016).
20. Lapinskas, T. et al. The intraventricular hemodynamic forces estimated using routine CMR cine images: A new marker of the failing heart. *JACC Cardiovasc. Imaging* **12**, 377–379 (2019).
21. Töger, J. et al. Intracardiac hemodynamic forces using 4D flow: A new reproducible method applied to healthy controls, elite athletes and heart failure patients. *J. Cardiovasc. Magn. Reson.* **18 (Suppl. 1)**, Q61 (2016).
22. Arvidsson, P. M. et al. Hemodynamic force analysis is not ready for clinical trials on HFpEF. *Sci. Rep.* **12**, 4017 (2022).
23. Arvidsson, P. M. et al. Hemodynamic forces using four-dimensional flow MRI: An independent biomarker of cardiac function in heart failure with left ventricular dyssynchrony? *Am. J. Physiol. Heart Circ. Physiol.* **315**, H1627–H1639 (2018).
24. Backhaus, S. J. et al. Hemodynamic force assessment by cardiovascular magnetic resonance in HFpEF: A case-control substudy from the HFpEF stress trial. *eBioMedicine* **86**, 104334 (2022).
25. Monosilio, S. et al. Cardiac and vascular remodeling after 6 months of therapy with sacubitril/valsartan: Mechanistic insights from advanced echocardiographic analysis. *Front. Cardiovasc. Med.* **9**, 883769 (2022).
26. Laenens, D. et al. Evolution of echocardiography-derived hemodynamic force parameters after cardiac resynchronization therapy. *Am. J. Cardiol.* **209**, 138–145 (2023).
27. Pola, K. et al. Hemodynamic forces from 4D flow magnetic resonance imaging predict left ventricular remodeling following cardiac resynchronization therapy. *J. Cardiovasc. Magn. Reson.* **25**, 45 (2023).
28. Faganello, G. et al. Impact of left ventricular hemodynamic forces in adult patients with treated aortic coarctation and preserved left ventricular systolic function. *Echocardiography* **41**, e15742 (2024).
29. Airale, L. et al. A novel approach to left ventricular filling pressure assessment: The role of hemodynamic forces analysis. *Front. Cardiovasc. Med.* **8**, 704909 (2021).
30. Filomena, D. et al. Hemodynamic forces in olympic athletes assessed by cardiac magnetic resonance: A new non-invasive screening tool? *Eur. J. Prev. Cardiol.* **29** (Suppl. 1) (2022).
31. Kawel-Boehm, N. et al. Reference ranges (normal values) for cardiovascular magnetic resonance (CMR) in adults and children: 2020 update. *J. Cardiovasc. Magn. Reson.* **22**, 87 (2020).

32. Hammond, I. W. et al. The prevalence and correlates of echocardiographic left ventricular hypertrophy among employed patients with uncomplicated hypertension. *J. Am. Coll. Cardiol.* **7**, 639–650 (1986).

Acknowledgements
This study was funded by a grant of the Ministry of Education and Science of the Republic of Kazakhstan, № AP14869730.

Author contributions
DJ: Data collection and analysis, writing initial draft; YR: Conceptualization, provision of patients; NK: Data collection and analysis; AZ: Data analysis, data curation, literature search; BT: Provision of patients, investigation, literature search; ZK: Data curation, formal analysis, statistics; NZ: Provision of patients, investigation, visualisation; MB: Provision of patients, instrumentation, computing resources; TD: Provision of patients, instrumentation, computing resources; AG: Conceptualization, design of methodology; GT: Data analysis; AS: Conceptualization, design of methodology, supervision, writing-review & editing. All authors had full access to the underlying data. All authors read and approved the final manuscript.

Declarations

Competing interests
The authors declare no competing interests.

Additional information
Correspondence and requests for materials should be addressed to A.S.

Reprints and permissions information is available at www.nature.com/reprints.

Publisher's note Springer Nature remains neutral with regard to jurisdictional claims in published maps and institutional affiliations.